Monthly Notices
of the
ROYAL ASTRONOMICAL SOCIETY

MNRAS **450,** 3958–3965 (2015) doi:10.1093/mnras/stv873

Optical flickering of the recurrent nova RS Ophiuchi: amplitude–flux relation*

R. Zamanov,[1†] G. Latev,[1†] S. Boeva,[1] J. L. Sokoloski,[2] K. Stoyanov,[1†] R. Bachev,[1] B. Spassov,[1] G. Nikolov,[1] V. Golev[3] and S. Ibryamov[1]

[1]*Institute of Astronomy and National Astronomical Observatory, Bulgarian Academy of Sciences, Tsarigradsko Shose No. 72, 1784 Sofia, Bulgaria*
[2]*Columbia Astrophysics Laboratory, Columbia University, 550 West 120th Street, New York, NY 10027, USA*
[3]*Department of Astronomy, Faculty of Physics, St Kliment Ohridski University of Sofia, 5 James Bourchier Blvd, 1164 Sofia, Bulgaria*

Accepted 2015 April 17. Received 2015 April 17; in original form 2015 January 7

ABSTRACT

We report observations of the flickering variability of the symbiotic recurrent nova RS Oph at quiescence in five bands (*UBVRI*). We find evidence of a correlation between the peak-to-peak flickering amplitude (ΔF) and the average flux of the hot component ($F_{\rm av}$). The correlation is highly significant, with a correlation coefficient of 0.85 and a p-value of $\sim 10^{-20}$. Combining the data from all wavebands, we find a dependence of the type $\Delta F \propto F_{\rm av}^{k}$, with power-law index $k = 1.02 \pm 0.04$ for the *UBVRI* flickering of RS Oph. Thus, the relationship between the amplitude of variability and the average flux of the hot component is consistent with linearity. The rms amplitude of flickering is on average 8 per cent (±2 per cent) of $F_{\rm av}$. The detected correlation is similar to that found in accreting black holes/neutron stars and cataclysmic variables. The possible reasons are briefly discussed. The data are available upon request from the authors.

Key words: accretion, accretion discs – binaries: symbiotic – stars: individual: RS Oph – novae, cataclysmic variables.

1 INTRODUCTION

In the symbiotic recurrent nova RS Ophiuchi (HD 162214), a near-Chandrasekhar-mass white dwarf (WD) accretes material from a red giant companion (e.g. Hachisu & Kato 2001; Sokoloski et al. 2006; Bode 2010, and references therein). It experiences nova eruptions approximately every 20 yr. RS Oph has undergone recorded outbursts in 1898, 1933, 1958, 1967, and 1985 (Rosino 1987), with a possible additional outburst in 1907 (Schaefer 2010). The most recent eruption occurred on 2006 February 12 (Narumi et al. 2006).

Using infrared radial velocity measurements, Fekel et al. (2000) found that RS Oph has an eccentricity $e \approx 0$ and that the red giant and WD have masses of 2.3 $M_\odot$ and close to 1.4 $M_\odot$, respectively, with a separation between the components of $a = 2.68 \times 10^{13}$ cm. Brandi et al. (2009), on the basis of optical and infrared spectra, derived a mass ratio $q = M_g/M_h = 0.59 \pm 0.05$ and fine-tuned the orbital period to 453.6 ± 0.4 d.

Worters et al. (2007) proposed that for the range of spectral types suggested for the red giant in the RS Oph system, its radius is smaller than its Roche lobe, and accretion on to the WD may occur only from the red giant wind. Wynn (2008) considered that both Roche lobe overflow and stellar wind capture are plausible methods for the accretion process in RS Oph. He also proposed that the accretion disc is probably a hybrid type with stable, cold outer regions and stable, hot inner regions (Wynn 2008). *Chandra* and *XMM–Newton* observations obtained after the 2006 outburst suggest that the mass accretion rate at that time was about 2×10^{-8} $M_\odot$ yr^{-1} (Nelson et al. 2011).

Flickering (aperiodic broad-band variability) is a type of variability observed in the three main classes of binaries that contain WDs accreting material from a companion mass-donor star: cataclysmic variables (CVs), supersoft X-ray binaries, and symbiotic stars (Sokoloski 2003). The flickering is not only observed in accreting WD, but also in accreting black holes and neutron stars (e.g. Belloni, Psaltis & van der Klis 2002, and references therein). The flickering of RS Oph has been detected by Walker (1977), among others. Systematic searches for flickering variability in symbiotic stars and related objects (Dobrzycka, Kenyon & Milone 1996; Sokoloski, Bildsten & Ho 2001; Gromadzki et al. 2006) have shown that among ∼200 known symbiotic stars, only 10 present flickering – RS Oph, T CrB, MWC 560, Z And, V2116 Oph, CH Cyg, RT

* Based on observations obtained in National Astronomical Observatory Rozhen and Belogradchik Observatory, Bulgaria.

† E-mail: rkz@astro.bas.bg (RZ); glatev@astro.bas.bg (GL); kstoyanov@astro.bas.bg (KS)

Cru, *o* Cet, and more recently V407 Cyg (Kolotilov et al. 2003) and V648 Car (Angeloni et al. 2012).

Here, we present new observations of the flickering variability of RS Oph in the *UBVRI* bands, and investigate the behaviour of the flickering amplitude.

2 OBSERVATIONS

Although some of the observations presented here were performed before the 2006 outburst using the 1.0 m Nickel telescope at UCO/Lick Observatory on Mt. Hamilton near San Jose, CA (USA), the majority were obtained between 2008 July and 2013 September with the 2 m RCC telescope, the 50/70 cm Schmidt telescope, the 60 cm telescope of the Bulgarian National Astronomical Observatory Rozhen, and the 60 cm telescope of the Belogradchick Astronomical Observatory. All of the telescopes are equipped with CCD cameras. The 2 m RCC telescope is equipped with a dual channel focal reducer (Jockers et al. 2000) and can observe simultaneously in two bands – *U* (blue channel) and *V* (red channel).

All of the CCD images have been bias subtracted and flat fielded, and standard aperture photometry has been performed. The data from Lick Observatory were reduced using IDL. For the data from Rozhen and Belogradchick, the reduction and aperture photometry were done with IRAF and checked with alternative software packages. Depending upon the field of view, we used between two and six comparison stars from the list of Henden & Munari (2006). Table 1 lists the date in format YYYY MMM DD, the telescope, band, UT-start, and UT-end of the run, exposure time, number of CCD images obtained, average magnitude in the corresponding band, minimum–maximum magnitudes in each band, standard deviation of the mean, and typical observational error. The exposure times were from 3 to 240 s, and the read-out-times were from 3 to 20 s, depending on the brightness of the object and the observational setup. The typical accuracy of the photometry was ∼0.01 mag (see Table 1 for the accuracy of the individual light curves).

In addition to the new observations, we also used published data (Zamanov & Bachev 2007; Zamanov et al. 2010). A few examples of our observations are presented in Fig. 1.

3 RED GIANT CONTRIBUTION

Pavlenko et al. (2008) modelled a 2006 August spectrum of RS Oph in the 1.4–2.5 μm range and determined the following parameters for the red giant: $T_{\rm eff} = 4100 \pm 100$ K, $\log g = 0.0 \pm 0.5$, $[{\rm Fe/H}] = 0.0 \pm 0.5$, $[{\rm C/H}] = -0.8 \pm 0.2$, and $[{\rm N/H}] = +0.6 \pm 0.3$. These abundances may vary considerably, however, if the red giant is contaminated by the nova ejecta, as has been suggested by Scott et al. (1994). Irradiation of the red giant by the still-hot WD may also be a complicating factor in the immediate aftermath of an eruption. Using near-infrared spectroscopy in the 1–5 μm range, Rushton et al. (2010) found $T_{\rm eff} = 4200 \pm 200$ K for the red giant.

The grids of colours for cool stars (Houdashelt, Bell & Sweigartet 2000) in Johnson–Cousins system (for $\log g = 0.0$, $[{\rm Fe/H}] = 0.0$) give for $T_{\rm eff} = 4000$: $U-V = 4.178$, $B-V = 1.725$, $V-R = 0.822$, and $V-I = 1.520$, and for $T_{\rm eff} = 4250$: $U-V = 3.731$, $B-V = 1.575$, $V-R = 0.723$, and $V-I = 1.325$. For the red giant of RS Oph, we assume $(U-V)_0 = 3.95$, $(B-V)_0 = 1.65$, $(V-R)_0 = 0.77$, and $(V-I)_0 = 1.42$.

Skopal (2015) modelled the spectral energy distribution of RS Oph adopting $V \sim 12.0$ for the red giant. Using decomposition of the spectrum of RS Oph in quiescence, Kelly et al. (2014) estimated that the giant star should be 0.65 mag fainter in *V* than the total magnitude of the binary system, which they suppose to be ∼11.5. This gives for the giant $V \approx 12.15$.

During the time of our observation, the *V* brightness of RS Oph varied between 10.093 and 11.633 mag. However, after the 2006 outburst the brightness of RS Oph achieved a minimum value $V \sim 12.25$ (AAVSO data; Henden 2013), which we take to be 99 per cent due to the red giant (because some contribution from the WD and nebula should exist). The red giant is 'perhaps slightly variable', as noted by Rosino, Bianchini & Rafanelli (1982) and Rushton et al. (2010). Scott et al. (1994) discussed a mechanism whereby the outbursts contaminate the red giant with excess carbon, which is subsequently convected away. This would have a negligible influence on the broad-band optical magnitudes of the red giant, and we assume that the red giant is non-variable in *UBVRI*. We adopt interstellar reddening towards RS Oph of $E(B-V) = 0.73$ (Snijders 1987).

4 FLICKERING QUANTITIES

We converted the magnitudes into fluxes, adopting fluxes for a zero-magnitude star of $F_0(U) = 4.167 \times 10^{-9}$, $F_0(B) = 6.601 \times 10^{-9}$, $F_0(V) = 3.610 \times 10^{-9}$, $F_0(R) = 2.256 \times 10^{-9}$, and $F_0(I) = 1.226 \times 10^{-9}$ erg cm^{-2} s^{-1} Å^{-1} (Bessell 1979). The observed flux during a given night was corrected for the contribution of the red giant and interstellar extinction. For each run, we calculate the following dereddened quantities:

$F_{\rm max}$ – the maximum flux of the hot component;
$F_{\rm min}$ – the minimum flux of the hot component;
$\Delta F = F_{\rm max} - F_{\rm min}$ – peak-to-peak amplitude of the flickering;
$F_{\rm av}$ – the average flux of the hot component:

$$F_{\rm av} = \frac{1}{N}\sum_{i=1}^{N} F_i; \quad (1)$$

$F_{\rm fl}$ – the average flux of the flickering, $F_{\rm fl} = F_{\rm av} - F_{\rm min}$;

and the absolute rms amplitude of variability (the square-root of the light-curve variance):

$$\sigma_{\rm rms_0} = \sqrt{\frac{1}{N-1}\sum_{i=1}^{N}(F_i - F_{\rm av})^2}, \quad (2)$$

where *N* is the number of the data points in the run (as used in Uttley, McHardy & Vaughan 2005). Subsequently, we subtract the contribution expected from measurement errors

$$\sigma_{\rm rms} = \sqrt{{\sigma_{\rm rms_0}}^2 - {\sigma_{\rm err}}^2}, \quad (3)$$

where $\sigma_{\rm err}$ is the mean observational error.

Following King et al. (2004), we calculate rms flux:

$$\sigma = \frac{1}{N}\sqrt{\sum_{i=1}^{N}(F_i - F_{\rm av})^2}. \quad (4)$$

We correct σ for the observational errors in a similar way as equation (3). The corrections of σ and $\sigma_{\rm rms}$ for the measurement errors are small, in the range 1–4 per cent.

In Fig. 2 are plotted the flickering quantities $F_{\rm max}$, $F_{\rm min}$, and $F_{\rm fl}$ versus the average flux of the hot component. The individual errors are also indicated (in most cases they are less than or equal to the size of the symbols). Although we expect them to be connected,

Table 1. CCD observations of RS Oph.

Date	Telescope	Band	UT start–end	Exp-time (s)	N_{pts}	Average (mag)	min–max (mag)-(mag)	stdev (mag)	err (mag)
1997 09 01	1 m Lick	*B*	03:41–06:53	22	233	12.297	12.078–12.444	0.068	0.005
1997 09 02	1 m Lick	*B*	03:29–06:49	22	238	12.484	12.305–12.653	0.086	0.005
1998 07 19	1 m Lick	*B*	05:34–08:43	60	128	12.392	12.182–12.617	0.108	0.004
1998 07 20	1 m Lick	*B*	05:02–08:38	60	149	12.235	12.089–12.389	0.071	0.003
1998 07 22	1 m Lick	*B*	07:01–08:59	60	82	12.109	11.978–12.404	0.076	0.003
2008 07 09	60 cm Roz	*V*	19:44–21:08	60	50	11.218	11.313–11.110	0.052	0.020
2009 06 14	60 cm Roz	*B*	23:35–00:32	30	70	11.722	11.605–11.855	0.060	0.020
2009 06 14	60 cm Roz	*I*	23:36–00:32	5	70	8.852	8.773–8.951	0.032	0.010
2009 06 14	60 cm Bel	*V*	23:37–00:43	20	95	10.703	10.557–10.817	0.049	0.005
2009 06 14	60 cm Bel	*R*	23:37–00:43	10	95	9.839	9.701–9.915	0.040	0.005
2009 06 15	60 cm Roz	*B*	22:24–00:03	40	81	11.858	11.714–12.045	0.062	0.010
2009 06 15	60 cm Roz	*I*	22:25–00:04	10	81	8.955	8.848–9.037	0.035	0.005
2009 06 15	60 cm Bel	*V*	23:31–01:02	20	130	10.795	10.693–10.934	0.046	0.005
2009 06 15	60 cm Bel	*R*	23:31–01:02	10	130	9.926	9.834–10.038	0.038	0.005
2010 04 30	60 cm Roz	*B*	22:47–00:19	30,60	65	11.737	11.603–11.848	0.059	0.006
2010 04 30	60 cm Roz	*V*	22:48–00:21	10	65	10.621	10.521–10.718	0.048	0.006
2010 05 01	60 cm Roz	*B*	22:19–00:19	60	68	11.431	11.121–11.612	0.128	0.004
2010 05 01	60 cm Roz	*V*	22:19–00:20	20	69	10.375	10.093–10.541	0.113	0.003
2010 05 02	60 cm Roz	*U*	22:42–00:25	120	30	11.576	11.354–11.739	0.118	0.013
2010 05 02	60 cm Roz	*B*	22:56–00:27	60	29	11.643	11.457–11.777	0.097	0.006
2012 04 27	70 cm Sch	*U*	00:07–01:34	60,120	54	12.037	11.850–12.244	0.086	0.011
2012 04 27	60 cm Roz	*B*	00:28–01:43	60	61	12.112	11.934–12.271	0.070	0.006
2012 04 27	60 cm Bel	*V*	00:03–01:39	20	141	10.982	10.876–11.120	0.052	0.006
2012 04 27	60 cm Roz	*I*	00:29–01:44	3	61	9.044	8.986–9.110	0.029	0.006
2012 06 13	60 cm Roz	*U*	21:45–23:36	120	33	12.599	12.407–12.762	0.089	0.014
2012 06 13	60 cm Roz	*B*	21:47–23:37	20	34	12.531	12.380–12.671	0.086	0.012
2012 06 13	60 cm Roz	*V*	21:43–23:37	10	34	11.376	11.274–11.492	0.063	0.007
2012 06 13	60 cm Roz	*R*	21:43–23:38	5	34	10.363	10.282–10.451	0.050	0.002
2012 06 13	60 cm Roz	*I*	21:44–23:38	3	33	9.266	9.172–9.342	0.037	0.005
2012 07 18	2.0 m Roz	*U*	21:02–22:54	300	21	12.673	12.567–12.814	0.065	0.008
2012 07 18	70 cm Sch	*B*	20:45–23:00	20	317	12.722	12.614–12.851	0.046	0.010
2012 07 18	2 m Roz	*V*	21:02–22:58	15	200	11.540	11.462–11.617	0.030	0.006
2012 07 21	60 cm Bel	*B*	18:59–22:42	30	219	12.593	12.377–12.794	0.073	0.014
2012 07 21	60 cm Bel	*V*	18:59–22:43	10	222	11.432	11.288–11.628	0.050	0.009
2012 07 21	60 cm Bel	*R*	19:00–22:43	5	222	10.422	10.257–10.524	0.038	0.006
2012 07 21	60 cm Bel	*I*	19:00–22:43	3	222	9.326	9.205–9.439	0.054	0.005
2012 08 15	60 cm Roz	*B*	18:41–21:10	60	83	12.904	12.618–13.208	0.216	0.009
2012 08 15	60 cm Roz	*R*	18:42–21:10	5	83	10.579	10.399–10.730	0.116	0.008
2012 08 15	60 cm Roz	*I*	18:42–21:10	5	83	9.404	9.301–9.501	0.065	0.006
2012 08 16	2.0 m Roz	*U*	18:48–20:51	180,240	28	12.782	12.659–12.904	0.070	0.022
2012 08 16	2.0 m Roz	*V*	18:47–20:51	10	224	11.563	11.472–11.633	0.037	0.004
2012 08 16	70 cm Sch	*B*	18:35–20:44	30	224	12.769	12.561–12.897	0.071	0.007
2013 07 02	60 cm Roz	*B*	20:41–22:43	60	46	12.196	11.982–12.368	0.074	0.008
2013 07 02	60 cm Roz	*V*	20:42–22:44	60	49	11.115	10.988–11.237	0.060	0.005
2013 07 10	70 cm Sch	*B*	21:23–23:42	30	126	12.033	11.887–12.207	0.069	0.008
2013 07 10	70 cm Sch	*V*	21:23–23:43	15	128	11.041	10.896–11.196	0.065	0.006
2013 08 12	2.0 m Roz	*U*	19:09–21:27	180	34	11.996	11.766–12.171	0.121	0.009
2013 08 12	70 cm Sch	*B*	18:50–21:30	15,20	470	12.129	11.916–12.270	0.083	0.012
2013 08 12	2.0 m Roz	*V*	19:12–21:30	3, 5	335	11.060	10.897–11.203	0.069	0.005
2013 08 12	60 cm Roz	*R*	19:17–21:29	3	285	10.129	9.985–10.240	0.057	0.007
2013 08 12	60 cm Roz	*I*	19:17–21:28	3	285	9.069	8.954–9.185	0.046	0.004
2013 08 13	2.0 m Roz	*U*	18:58–21:21	180	37	12.487	12.296–12.658	0.101	0.013
2013 08 13	70Sch+60Roz	*B*	20:40–21:22	20	92	12.579	12.476–12.659	0.042	0.010
2013 08 13	2.0 m Roz	*V*	18:58–21:22	3	362	11.391	11.274–11.503	0.060	0.004
2013 08 13	60 cm Roz	*R*	18:48–21:21	3	320	10.365	10.265–10.467	0.046	0.008
2013 08 13	60 cm Roz	*I*	18:48–21:21	3	320	9.197	9.107–9.288	0.038	0.005
2013 09 05	60 cm Bel	*B*	18:45–19:47	30	52	12.033	11.864–12.226	0.086	0.015
2013 09 05	60 cm Bel	*V*	18:46–19:47	10	51	10.866	10.730–11.028	0.074	0.010
2013 09 05	60 cm Bel	*R*	18:46–19:47	3	51	9.933	9.819–10.082	0.067	0.015
2013 09 05	60 cm Bel	*I*	18:46–19:48	3	51	8.983	8.875–9.091	0.052	0.015
2013 09 06	60 cm Bel	*B*	18:41–19:25	30	39	12.012	11.848–12.152	0.090	0.006
2013 09 06	60 cm Bel	*V*	18:41–19:25	10	39	10.865	10.723–10.977	0.071	0.004
2013 09 06	60 cm Bel	*R*	18:42–19:25	5	39	9.889	9.786–9.960	0.047	0.003
2013 09 06	60 cm Bel	*I*	18:42–19:25	5	39	8.971	8.868–9.047	0.043	0.003

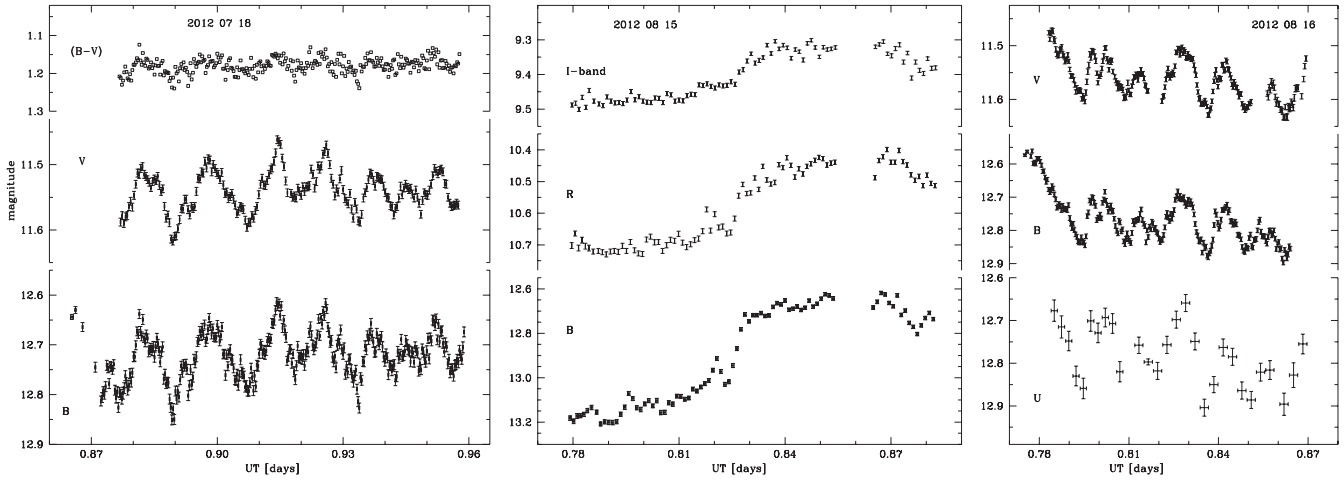

Figure 1. Example light curves of RS Oph.

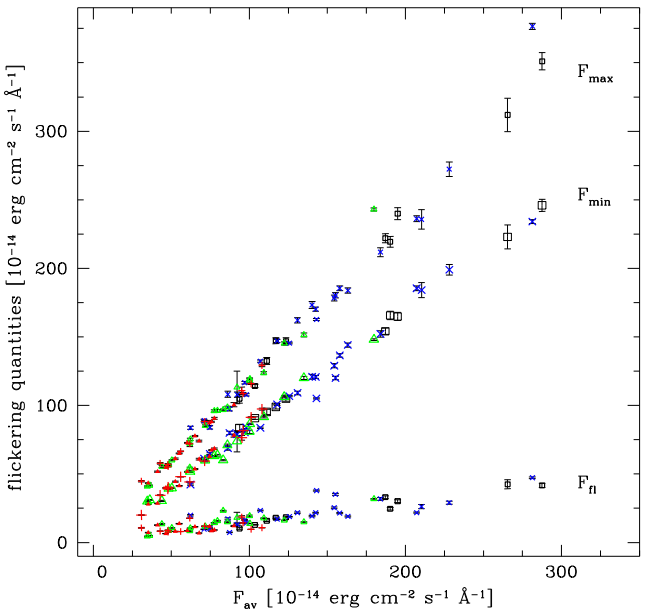

Figure 2. Measured flickering quantities $F_{\rm max}$, $F_{\rm min}$, and $F_{\rm fl}$ versus the average flux, $F_{\rm av}$, of the hot component. The symbols are U – black squares, B – blue crosses, V – green open triangles, R – red plusses, I – red filled triangles. The individual error bars are plotted in black.

it is not clear a priori how the different quantities depend on each other. Least-squares fit to data (taking into account the errors of the individual points) in Fig. 2 give

$$F_{\rm max} = 1.31\,(\pm1.64) + 1.161\,(\pm0.013)\ F_{\rm av}, \quad (5)$$

$$F_{\rm min} = -0.90\,(\pm1.17) + 0.857\,(\pm0.009)\ F_{\rm av}, \quad \text{and} \quad (6)$$

$$F_{\rm fl} = -0.33\,(\pm0.19) + 0.135\,(\pm0.002)\ F_{\rm av}, \quad (7)$$

where the units for all quantities are $10^{-14}\,{\rm erg\,cm^{-2}\,s^{-1}}$ Å. The relations (equations 5, 6, and 7) are very similar to those calculated for the recurrent nova T CrB (Zamanov et al. 2004).

5 RESULTS

5.1 Relationship between ΔF and $F_{\rm av}$

From the amplitude of the flickering versus the average flux plotted in Fig. 3(a), it is clear that ΔF increases with $F_{\rm av}$. We performed Pearson's correlation test and Spearman's (rho) rank correlation test. The results of these tests (correlation coefficient and p-value) are summarized in Table 2, where the first column lists the band(s) used, the second column the number of observations, the third the power-law index and its error, the fourth Pearson's correlation coefficient, and the fifth and sixth Spearman's correlation coefficient and its significance (p-value). The correlation between ΔF and $F_{\rm av}$ is highly significant ($p \ll 0.001$) even for a single band. Because the significance depends on the number of data points, we obtain higher significance when we use more data, achieving $p \sim 10^{-20}$, when we use all 73 light curves in *UBVRI* bands.

Our runs had durations from 40 min to 3 h, and the differing durations could in principle affect the behaviour of the flickering amplitude (because for red noise, rms amplitude depends on the time interval over which it is measured). To check that the differing light-curve durations were not influencing our results, we divided our B-band data into 1 h segments. We re-calculated sigma and amplitude. The result was similar to that obtained with the complete light curves (see Fig. 3 d, e, f, and Table 2).

Looking for a dependence of the type $\Delta F \propto F_{\rm av}^{k}$, we fit the data to a straight line in log–log space, taking errors into account (Fig. 4). The results for the power-law index k are summarized in the third column of Table 2. For the power-law index k, the calculated values are in the range $1.02 \leq k \leq 1.32$. In general, $k = 1.02 \pm 0.04$, which is derived from all of the observations, should provide a better measure of power-law index.

5.2 Relationship between rms variability and average flux

The rms variability (σ, $\sigma_{\rm rms}$) and $F_{\rm av}$ are also strongly correlated. Using all five bands for the correlation between σ and $F_{\rm av}$ (Fig. 3b), we calculate a correlation coefficient of 0.80 and a significance of $p = 3 \times 10^{-14}$. For $\sigma_{\rm rms}$ and $F_{\rm av}$ (Fig. 3c), we calculate a correlation coefficient of 0.84 and a significance of $p = 6 \times 10^{-17}$. The relationship between the rms variability and the mean flux is consistent with a linear dependance.

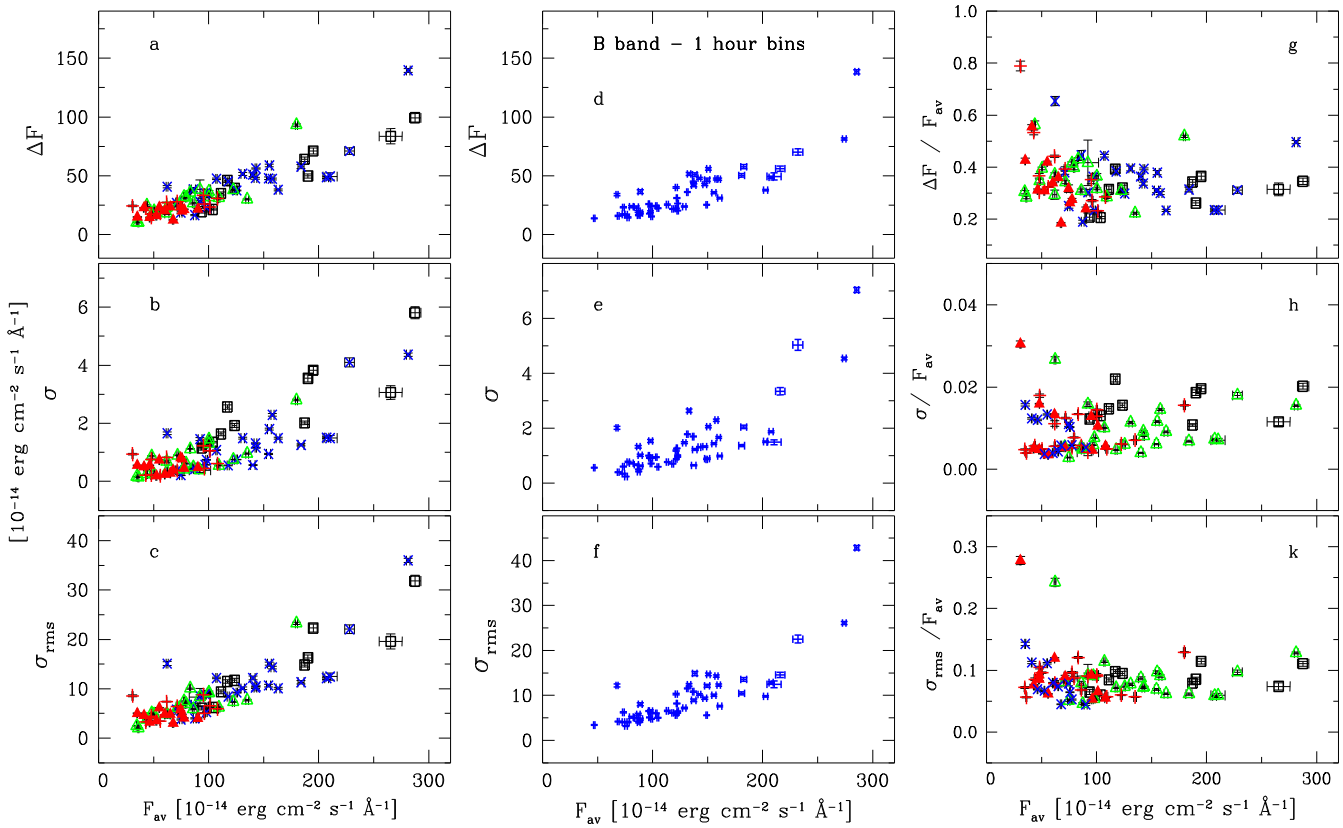

Figure 3. RS Oph: amplitude of the flickering versus the dereddened average flux of the hot component in *UBVRI* band. The symbols are the same as in Fig. 2. In (a), (b), and (c) panels are plotted amplitude ΔF, σ, and $\sigma_{\rm rms}$, respectively. In (d), (e), and (f) panels are plotted ΔF, σ, and $\sigma_{\rm rms}$ for 1 h bins. In (g), (h), and (k) panels is the normalized variability.

Table 2. Correlation analysis for the relationship between amplitude of flickering and the average flux of the hot component. In the table are given the band(s) used, $N_{\rm obs}$ (the number of light curves), power-law index k, Pearson and Spearman rank correlation coefficients, and their significance.

Bands	$N_{\rm obs}$	k	$r_{\rm P}$	$r_{\rm S}$	p-value
UBVRI	73	1.02 ± 0.04	0.88	0.86	2×10^{-23}
B	23	1.27 ± 0.12	0.83	0.80	5×10^{-6}
B 1 h bins	52	1.32 ± 0.08	0.84	0.83	3×10^{-14}
V	19	1.11 ± 0.08	0.88	0.80	2×10^{-5}
UB	33	1.31 ± 0.10	0.87	0.87	6×10^{-11}
BV	42	1.05 ± 0.05	0.89	0.87	5×10^{-14}
UBV	52	1.06 ± 0.05	0.89	0.88	6×10^{-18}

In Figs 3(g), (h), and (k) (right-hand panels), we plot the fractional variability, i.e. the variability normalized by $F_{\rm av}$. There are a few deviating points (the deviation is most clearly visible in Fig. 3k), which are due to 20150815 run (see Section 6.1 for details). We estimate mean values $<\sigma_{\rm rms}/F_{\rm av}> = 0.08 \pm 0.02$ and $<\sigma/F_{\rm av}> = 0.010 \pm 0.004$. Our data show that the fractional rms variability remains approximately constant, despite significant flux changes (∼factor of 4.4 in *B* band). Following King et al. (2004), $\sigma/F_{\rm av}$ depends on the Shakura & Sunyaev (1973) α-viscosity parameter in the accretion disc (see section 3.2.2 of King et al. 2004). For RS Oph, we calculate $\sigma/F_{\rm av} \sim 0.01$, which corresponds to $\alpha \leq 0.006$.

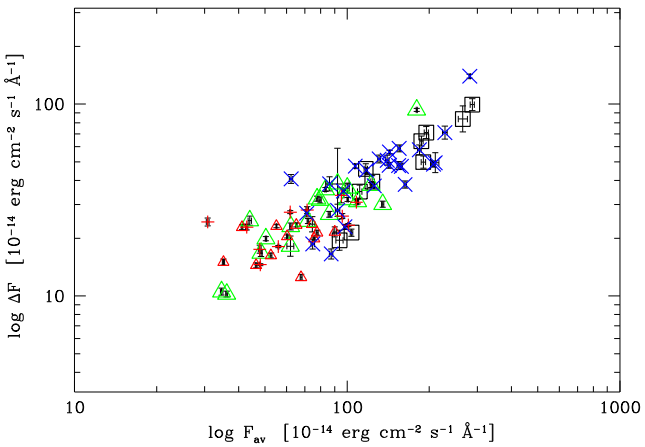

Figure 4. RS Oph: amplitude of the flickering versus the average flux in *UBVRI* bands, on a logarithmic scale. For the majority of points, the individual errors are less than or equal to the size of the symbols. The symbols are the same as in Fig. 2.

5.3 Flux distribution

A characteristic of the X-ray variability in X-ray binaries and active galaxies is the lognormal flux distribution (Uttley et al. 2005). This distribution is also found in the *Kepler* observations of V1504 Cyg and KIC 8751494 (Van de Sande, Scaringi & Knigge 2015).

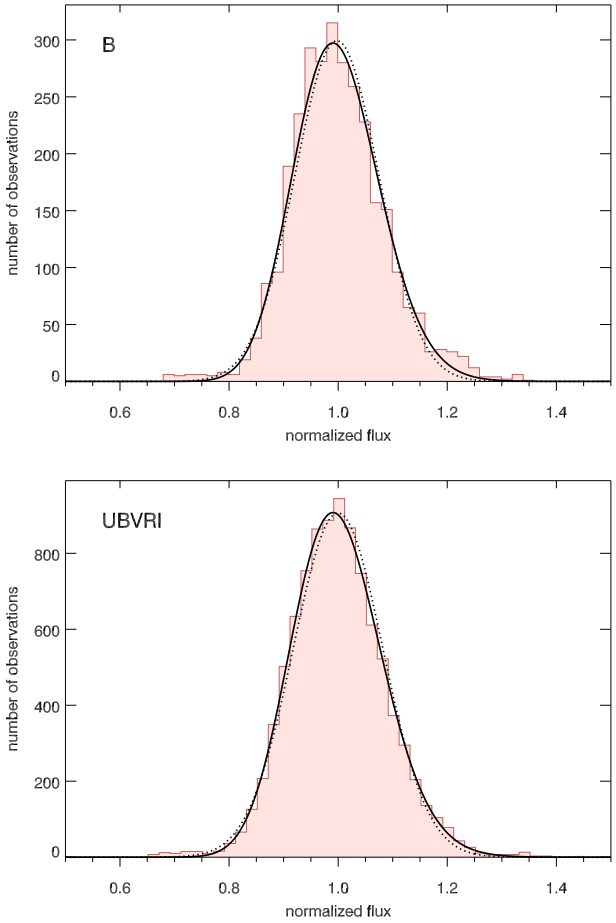

Figure 5. Flux distribution of RS Oph, *B*-band data (upper panel), and all *UBVRI* data (lower panel). Scott's normal reference rule was used to determine the binsize of 0.02, because it is optimal for random samples of normally distributed data. Lognormal distribution fits are drawn with solid lines, the dotted lines represent Gaussian distribution fits.

To check whether RS Oph exhibits a similar behaviour, we performed both Gaussian and lognormal fits to the flux distribution of the *B*-band data and to all of the *UBVRI* data (Fig. 5). For the *B*-band data the fit to the normal (Gaussian) distribution gives reduced $\chi 2 = 4.53$ (centre of the distribution 0.9977, standard deviation 0.0768, degrees of freedom 31). The lognormal distribution fit with lognormal centre of 0.9997 and lognormal standard deviation of 0.0792 gives reduced $\chi 2 = 3.06$ (degrees of freedom 31). For *UBVRI* sample the normal distribution fit (centre 0.9997, standard deviation 0.0822) gives reduced $\chi 2 = 4.82$ (degrees of freedom 37), while the lognormal distribution fit gives reduced $\chi 2 = 2.51$ (lognormal centre of 1.0008 and lognormal standard deviation of 0.0835, degrees of freedom 37).

The results show that the lognormal distribution provides a better fit to the flux distribution of RS Oph in the optical bands because it better accounts for the skew.

6 DISCUSSION

The flickering of RS Oph disappeared after the 2006 outburst (Zamanov et al. 2006), indicating that the accretion disc was destroyed by the blast wave from the nova. Photometric data of Worters et al. (2007) showed evidence of the resumption of optical flickering, indicating reestablishment of accretion by day 241 of the outburst. Most of the present data were obtained after the reappearance of the flickering. That the data obtained before and after the outburst (1997–1998) and (2009–2013) exhibit the same behaviour confirms that the behaviour we see persists over long time periods (more than a decade).

6.1 Light curve from 2012 August 15

Kundra, Hric & Gális (2010) performed wavelet analysis of the flickering of RS Oph and found two different sources of flickering, the first with amplitude 0.1 mag and frequencies of 60–100 cycles d^{-1}, and the second with amplitude 0.6 mag and frequencies of less than 50 cycles d^{-1}. These frequencies are also visible in most of our observations (Fig. 1, left-hand and right-hand panels). However, they are not visible in our 20120815 run (see Fig. 1, mid panel). The light curve of RS Oph obtained on 2012 August 15 shows smooth variations. It resembles the *B*-band light curve of CH Cyg obtained on 1997 June 9 (see fig. 1 of Sokoloski & Kenyon 2003b), during which time Sokoloski & Kenyon (2003a) suggested that the inner disc was disrupted due to the launch of a jet. The fractional rms variability during this run was $\sigma_{\rm rms}/F_{\rm av} = 0.23$. This value deviates considerably from that of other runs (see Fig. 3f), indicating that at this moment the accretion disc was in an unusual state.

6.2 Amplitude of flickering

We detect (Section 5.1) correlation between ΔF and $F_{\rm av}$. Such a correlation has already been detected in few other binaries. Analysing the *U*-band flickering of the symbiotic star CH Cyg in 1974–1989, Mikolajewski et al. (1990) found that the amplitude of the flickering in *U*-band is a power-law function of the flux, $\Delta F \sim F^k$, with $1.40 < k < 1.45$. For the recurrent nova T CrB, Zamanov et al. (2004) estimated $k = 1.03$–1.09, and for the nova-like CV star KR Aur, Boeva et al. (2007) gave $k = 0.70$–0.75.

Our results for RS Oph point to a value of $k = 1.02 \pm 0.04$, not surprisingly similar to the value derived in T CrB. There are many similarities between these two 'sister' systems, e.g. they both: (1) are recurrent novae; (2) harbour very massive WDs; and (3) accrete at similar rates – RS Oph: 2×10^{-8} $M_\odot$ yr^{-1} (Nelson et al. 2011), T CrB: 2.5×10^{-8} $M_\odot$ yr^{-1} (Selvelli & Gilmozzi 1999).

An increase in brightness (and $F_{\rm av}$) is usually due to an increase in the mass accretion rate. If the flickering is coming from the boundary layer between the accretion disc and the WD (innermost part of the accretion disc), we expect the correlations between $F_{\rm av}$ and other quantities ($F_{\rm min}$, $F_{\rm max}$, $F_{\rm fl}$, ΔF, $\sigma_{\rm rms}$) to be connected with the response (changes in the structure and/or the size) of the boundary layer to the changes in $\dot{M}_{\rm acc}$. If the flickering is coming from a hotspot (outer part of the accretion disc), we expect the correlations to be associated with the size (mass) of the accreting blobs.

Dobrotka et al. (2010) analysed *V*-band photometry of the aperiodic variability in T CrB. By applying a prescription for angular momentum transport in the accretion disc, they developed a method to simulate the statistical distribution of flare durations under the assumption that the aperiodic variability is produced by turbulent elements in the disc. Furthermore, the simulated light curves (Dobrotka, Mineshige & Ness 2015) exhibit the typical linear rms–flux relation and lognormal distribution.

In CVs, many statistical properties of the flickering are explained with the fluctuating accretion disc model in which variations in the mass transfer rate through the disc are modulated on the local

viscous time-scale and propagate towards the central compact object (Scaringi 2014). Alternatively, Yonehara, Mineshige & Welsh (1997) proposed a model in which light fluctuations are produced by occasional flare-like events and subsequent avalanche flow in the accretion disc atmospheres. Flares are assumed to be ignited when the mass density exceeds a critical density. In this model, the correlations could be connected with the size of the element, where the density exceeds a critical density.

6.3 Analogy with accreting black holes

One feature of the broad-band X-ray variability of accreting black holes is the so-called rms–flux relation, which is a linear relationship between the absolute rms amplitude of variability and the flux, such that sources become more variable as they get brighter. Uttley & McHardy (2001) found this relation in Cyg X-1 (black hole mass 14.8 $M_{\odot}$; Orosz et al. 2011) and in the accreting millisecond pulsar SAX J1808.4-3658 (neutron star mass $\approx$2 $M_{\odot}$; Wang et al. 2013). Heil & Vaughan (2010) reported the detection of this relation in the ultraluminous X-ray source NGC 5408 X-1 (black hole mass 100–1000 $M_{\odot}$).

A similar linear relationship between the rms variability amplitude and the mean flux was discovered in the CVs MV Lyrae (Scaringi et al. 2012), V1504 Cyg, and KIC8751494 (Van de Sande et al. 2015). In MV Lyr, the WD mass is $\approx$0.72 $M_{\odot}$, and the mass transfer rate ranges from 3×10^{-13} $M_{\odot}$ yr^{-1} (Hoard et al. 2004) to 8.5×10^{-10} $M_{\odot}$ yr^{-1} (Echevarría 1994) and 2×10^{-9} $M_{\odot}$ yr^{-1} (Godon & Sion 2011). The observations reported here indicate that a similar relationship exists in the case of RS Oph, although in RS Oph the WD mass is close to the Chandrasekar limit (Brandi et al. 2009) and the mass accretion rate is a few orders of magnitude higher 2×10^{-7}–2×10^{-8} $M_{\odot}$ yr^{-1} (Osborne et al. 2011; Nelson et al. 2011).

The rms–flux relation remains an enigmatic observational feature of accreting compact objects, but it clearly contains information about the dynamics of the infalling material. The similarities between the behaviour of the optical flickering amplitude in WD accretors and the X-ray variability of accreting black holes indicate that similar processes may produce the short-term variability in the accretion flows around WDs, stellar mass black holes, and supermassive black holes. The deviating points (like 20120815) could help us to better understand the physical processes producing the short-term variability.

7 CONCLUSIONS

We present observations of the flickering variability of the recurrent nova RS Oph at quiescence in the optical *UBVRI* bands. We find a highly significant correlation between the flickering amplitude and the average flux of the hot component. We estimated the relation between the average flux of the hot component and various flickering quantities ($F_{\rm min}$, $F_{\rm max}$, $F_{\rm fl}$, ΔF, $\sigma_{\rm rms}$). The amplitude–flux (ΔF versus $F_{\rm av}$) and rms–flux (σ versus $F_{\rm av}$) as well as the other relations contain information about the infalling material in the accretion disc and should be useful to test the theoretical models of flickering.

ACKNOWLEDGEMENTS

This work is partially supported by the OP 'HRD', ESF and Bulgarian Ministry of Education and Science (BG051PO001-3.3.06-0047). JLS acknowledges support from NSF grant AST-1217778.

REFERENCES

Angeloni R., Di Mille F., Ferreira Lopes C. E., Masetti N., 2012, ApJ, 756, L21
Belloni T., Psaltis D., van der Klis M., 2002, ApJ, 572, 392
Bessell M. S., 1979, PASP, 91, 589
Bode M. F., 2010, Astron. Nachr., 331, 160
Boeva S., Zamanov R. K., Antov A., Bachev R., Georgiev T. B., 2007, Bulg. Astron. J., 9, 11
Brandi E., Quiroga C., Mikołajewska J., Ferrer O. E., García L. G., 2009, A&A, 497, 815
Dobrotka A., Hric L., Casares J., Shahbaz T., Martnez-Pais I. G., Muñoz-Darias T., 2010, MNRAS, 402, 2567
Dobrotka A., Mineshige S., Ness J.-U., 2015, MNRAS, 447, 3162
Dobrzycka D., Kenyon S. J., Milone A. A. E., 1996, AJ, 111, 414
Echevarría J., 1994, Rev. Mex. Astron. Astrofis., 28, 125
Fekel F. C., Joyce R. R., Hinkle K. H., Skrutskie M. F., 2000, AJ, 119, 1375
Godon P., Sion E. M., 2011, PASP, 123, 903
Gromadzki M., Mikolajewski M., Tomov T., Bellas-Velidis I., Dapergolas A., Galan C., 2006, Acta Astron., 56, 97
Hachisu I., Kato M., 2001, ApJ, 558, 323
Heil L. M., Vaughan S., 2010, MNRAS, 405, L86
Henden A. A., 2013, Observations from the AAVSO International Database, available at: http://www.aavso.org
Henden A., Munari U., 2006, A&A, 458, 339
Hoard D. W., Linnell A. P., Szkody P., Fried R. E., Sion E. M., Hubeny I., Wolfe M. A., 2004, ApJ, 604, 346
Houdashelt M. L., Bell R. A., Sweigart A. V., 2000, AJ, 119, 1448
Jockers K. et al., 2000, Kinematika Fiz. Nebesnykh Tel Suppl., 3, 13
Kelly P. L. et al., 2014, ApJ, 790, 3
King A. R., Pringle J. E., West R. G., Livio M., 2004, MNRAS, 348, 111
Kolotilov E. A., Shenavrin V. I., Shugarov S. Y., Yudin B. F., 2003, Astron. Rep., 47, 777
Kundra E., Hric L., Gális R., 2010, in Prša A., Zejda M., eds, ASP Conf. Ser. Vol. 435, Binaries - Key to Comprehension of the Universe. Astron. Soc. Pac., San Francisco, p. 341
Mikolajewski M., Mikolajewska J., Tomov T., Kulesza B., Szczerba R., 1990, AcA, 40, 129
Narumi H., Hirosawa K., Kanai K., Renz W., Pereira A., Nakano S., Nakamura Y., Pojmanski G., 2006, IAU Circ., 8671, 2
Nelson T., Mukai K., Orio M., Luna G. J. M., Sokoloski J. L., 2011, ApJ, 737, 7
Orosz J. A., McClintock J. E., Aufdenberg J. P., Remillard R. A., Reid M. J., Narayan R., Gou L., 2011, ApJ, 742, 84
Osborne J. P. et al., 2011, ApJ, 727, 124
Pavlenko Y. V. et al., 2008, A&A, 485, 541
Rosino L., 1987, in Bode M. F., ed., RS Ophiuchi (1985) and the Recurrent Nova Phenomenon. VNU Science Press, Ho Chi Minh City, p. 1
Rosino L., Bianchini A., Rafanelli P., 1982, A&A, 108, 243
Rushton M. T. et al., 2010, MNRAS, 401, 99
Scaringi S., 2014, MNRAS, 438, 1233
Scaringi S., Körding E., Uttley P., Knigge C., Groot P. J., Still M., 2012, MNRAS, 421, 2854
Schaefer B. E., 2010, ApJ, 187, 275
Scott A. D., Rawlings J. M. C., Krautter J., Evans A., 1994, MNRAS, 268, 749
Selvelli P., Gilmozzi R., 1999, Mem. Soc. Astron. Ital., 70, 565
Shakura N. I., Sunyaev R. A., 1973, A&A, 24, 337
Skopal A., 2015, New Astron., 34, 123
Snijders M. A. J., 1987, Ap&SS, 130, 243
Sokoloski J. L., 2003, in Corradi R. L. M., Mikolajewska R., Mahoney T. J., eds, ASP Conf. Ser. Vol. 303, Symbiotic Stars Probing Stellar Evolution. Astron. Soc. Pac., San Francisco, p. 202
Sokoloski J. L., Kenyon S. J., 2003a, ApJ, 584, 1021
Sokoloski J. L., Kenyon S. J., 2003b, ApJ, 584, 1027
Sokoloski J. L., Bildsten L., Ho W. C. G., 2001, MNRAS, 326, 553
Sokoloski J. L., Luna G. J. M., Mukai K., Kenyon S. J., 2006, Nature, 442, 276

Uttley P., McHardy I. M., 2001, MNRAS, 323, L26
Uttley P., McHardy I. M., Vaughan S., 2005, MNRAS, 359, 345
Van de Sande M., Scaringi S., Knigge C., 2015, MNRAS, 448, 2430
Walker A. R., 1977, MNRAS, 179, 587
Wang D. H., Chen L., Zhang C. M., Lei Y. J., Qu J. L., 2013, MNRAS, 435, 3494
Worters H. L., Eyres S. P. S., Bromage G. E., Osborne J. P., 2007, MNRAS, 379, 1557
Wynn G., 2008, in Evans A, Bode M., O'Brien T. J., Darnley M. J., eds, ASP Conf. Ser. Vol. 401, RS Ophiuchi (2006) and the Recurrent Nova Phenomenon. Astron. Soc. Pac., San Francisco, p. 73
Yonehara A., Mineshige S., Welsh W. F., 1997, ApJ, 486, 388
Zamanov R. K., Bachev R., 2007, Astron. Telegram, 1220, 1
Zamanov R., Bode M. F., Stanishev V., Martí J., 2004, MNRAS, 350, 1477
Zamanov R., Boer M., Le Coroller H., Panov K., 2006, Inf. Bull. Var. Stars, 5733, 1
Zamanov R. K. et al., 2010, MNRAS, 404, 381

This paper has been typeset from a TEX/LATEX file prepared by the author.